5-2019

Manufacturing and Testing the Permanent Magnet Linear Motor

Renjie Kang
Linfield College

Manufacturing and Testing the Permanent Magnet Linear Motor

Renjie Kang

A THESIS

Submitted to

The Department of Physics

Linfield College

McMinnville, Oregon

In partial fulfillment

of the requirements for the degree of

BACHELOR OF SCIENCE

May, 2019

THESIS COPYRIGHT PERMISSIONS

Please read this document carefully before signing. If you have questions about any of these permissions, please contact the DigitalCommons Coordinator.

Title of the Thesis:

Manufacturing and Testing the permanent Magnet Linear Motor

Author's Name: (Last name, first name)

Kang, Renjie

Advisor's Name

Xie, Tianbao.

DigitalCommons@Linfield (DC@L) is our web-based, open access-compliant institutional repository for digital content produced by Linfield faculty, students, staff, and their collaborators. It is a permanent archive. By placing your thesis in DC@L, it will be discoverable via Google Scholar and other search engines. Materials that are located in DC@L are freely accessible to the world; however, your copyright protects against unauthorized use of the content. Although you have certain rights and privileges with your copyright, there are also responsibilities. Please review the following statements and identify that you have read them by signing below. Some departments may choose to protect the work of their students because of continuing research. In these cases, the project is still posted in the repository but content will only be accessible by individuals who are part of the Linfield community.

CHOOSE THE STATEMENT BELOW THAT DEFINES HOW YOU WANT TO SHARE YOUR THESIS. THE FIRST STATEMENT PROVIDES THE MOST ACCESS TO YOUR WORK; THE LAST STATEMENT PROVIDES THE LEAST ACCESS. CHOOSE ONLY ONE STATEMENT.

K.M.S. via email

RK I **agree** to make my thesis available to the Linfield College community and to the larger scholarly community upon its deposit in our permanent digital archive, DigitalCommons@Linfield, or its successor technology. My thesis will also be available in print at Nicholson Library and can be shared via interlibrary loan.

OR

RK I **agree** to make my thesis available **only** to the Linfield College community upon its deposit in our permanent digital archive, DigitalCommons@Linfield, or its successor technology. My thesis will also be available in print at Nicholson Library and can be shared via interlibrary loan.

OR

RK I **agree** to make my thesis available in print at Nicholson Library, including access for interlibrary loan.

OR

RK I **agree** to make my thesis available in print at Nicholson Library only.

Updated April 25, 2018

NOTICE OF ORIGINAL WORK AND USE OF COPYRIGHT-PROTECTED MATERIALS:

If your work includes images that are not original works by you, you must include permissions from the original content provider or the images will not be included in the repository. If your work includes videos, music, data sets, or other accompanying material that is not original work by you, the same copyright stipulations apply. If your work includes interviews, you must include a statement that you have the permission from the interviewees to make their interviews public. For information about obtaining permissions and sample forms, see https://copyright.columbia.edu/basics/permissions-and-licensing.html.

NOTICE OF APPROVAL TO USE HUMAN OR ANIMAL SUBJECTS:

If your research includes human subjects, you must include a letter of approval from the Linfield Institutional Review Board (IRB); see https://www.linfield.edu/faculty/irb.html for more information. If your research includes animal subjects, you must include a letter of approval from the Linfield Animal Care & Use Committee.

NOTICE OF SUBMITTED WORK AS POTENTIALLY CONSTITUTING AN EDUCATIONAL RECORD UNDER FERPA:

Under FERPA (20 U.S.C. § 1232g), this work may constitute an educational record. By signing below, you acknowledge this fact and expressly consent to the use of this work according to the terms of this agreement.

BY SIGNING THIS FORM, I ACKNOWLEDGE THAT ALL WORK CONTAINED IN THIS PAPER IS ORIGINAL WORK BY ME OR INCLUDES APPROPRIATE CITATIONS AND/OR PERMISSIONS WHEN CITING OR INCLUDING EXCERPTS OF WORK(S) BY OTHERS.

IF APPLICABLE, I HAVE INCLUDED AN APPROVAL LETTER FROM THE IRB TO USE HUMAN SUBJECTS OR FROM ANIMAL CARE & USE TO USE ANIMAL SUBJECTS.

Signature Signature redacted Date 5/20/2019

Printed Name Renjie Kang

Approved by Faculty Advisor Signature redacted Date 5/20/2019

Updated April 25, 2018

Thesis Acceptance

Linfield College

Thesis title:	Manufacturing and Testing the Permanent Magnet Linear Motor
Submitted by:	Renjie Kang
Date submitted:	May 16, 2019

Thesis Advisor: Signature redacted

Dr. Tianbao Xie

Physics Department: Signature redacted

Dr. Michael S. Crosser

Physics Department: Signature redacted

Dr. Jennifer Heath

Abstract

Controlled mechanical motion is vital in many useful applications in technology. Among them, linear motors have advantages over traditional rotating motors. In this work, we have built a permanent magnet linear motor to test and measure its energy efficiency. A maximum 29% total energy efficiency, and 67% energy transfer rate were detected. In addition, a C shape support structure is added to the moving part in order to increase the moving accuracy. The tests show that, with the support structure, the fluctuation in the vertical direction decreases significantly, but the friction of the system slightly increases.

Table of Contents

List of Figures

List of Tables

I. Introduction

Like conventional rotating motors, a linear motor is also an electric motor. A regular rotating motor has a static outer shell and a rotor, and it generates torque. Unlike the rotating motor, a linear motor has a stator (fixed base) and a mover (the moving component), and outputs thrust force directly[1]. Compared to rotating motors, linear motors have advantages in terms of size, thrust force, and acceleration[2], but it can be challenging to satisfying all the requirements, which include keeping the system in a small size, having great thrust force and having a reasonable low cost. Thus, in this project, a comparison of moving accuracy and energy efficiency between two mover structures is made to provide suggestions about improving the performance of linear motors with this structure.

Linear motors are used in a lot of industrial and military situations. For instance, in industrial manufacturing, linear motors can be found in CNC machines (Computer Numeric Control) which are utilized in precise cutting, carving, milling, and so on[3] [4]. In order to manufacture high precision components, the thrust motor must move with great moving accuracy. Traditionally, to realize the motion in one dimension requires a gear set and a rotating step motor[5]. However, when the rotor rolls back and forth, the unavoidable gaps between gears would result in a fluctuation. For this reason, linear motors are widely used in situations like this instead of conventional rotating motors[6]. Also, the conversion from the rotation to linear means that for practical purposes, there is a maximum speed. For this reason, linear motors are used to launch aircrafts on the aircraft carriers. Due to the limitation of carriers' size, aircrafts cannot accelerate to the takeoff speed on such short runways. Thus, secondary accelerators, linear

motors, are required to provide larger kinetic energy to aircrafts so that they can reach the takeoff speed with a short accelerating length.

The structure of linear motors seems to be distinct from the structure of rotating motors, but they can be considered as having similar fundamental compositions. It may help to imagine that the linear motor is expanded from a rotating motor. As Figure 1 shows below, red and blue blocks are the north and south poles of permanent magnets, yellow, green, and orange components are electromagnets.

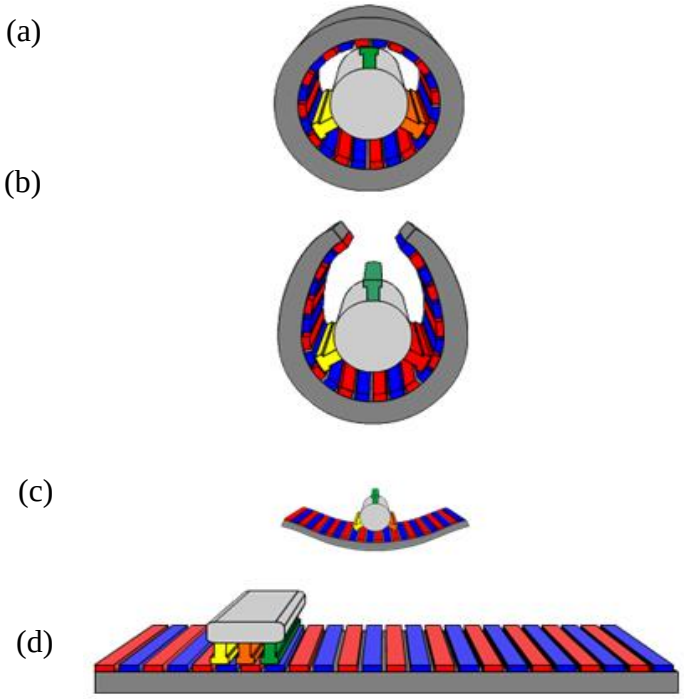

Figure 1: Correspondence between the operation of a rotating motor and a linear motor. Process of a rotating motor expands to a linear motor. (a) A common structure of a rotating motor, (b) and (c) two intermediate structures, (d) a linear motor. Reprinted from Wikimedia, by Shcnibbi678, 2013, Retrieved from: https://commons.wikimedia.org/wiki/File:Linearmotorprinzip.png. Copyright 2013 by Shcnibbi678. Reprinted with permission.

The stator part of the linear motor consists of an array of permanent magnets. (Figure 1 (d)). By sending current through the coil on the mover, a force is generated, according to the magnetic force equation, and as $q = it$ and $t = \frac{L}{v}$.

$$F = q\boldsymbol{v} \times \boldsymbol{B} = i\boldsymbol{L} \times \boldsymbol{B} \quad (1)$$

Here, the *v* is the velocity of the moving charge *q*, the B is the strength of the magnetic field generated by the permanent magnets array, *i* is the current and L is the length of the shorter side of the coil. As Figure 2 shows, the forces acting on the left and right parts of the coil (mover part in the linear motor, green component in Figure 2) would combine to a net force which can drive the rotator part to move left.

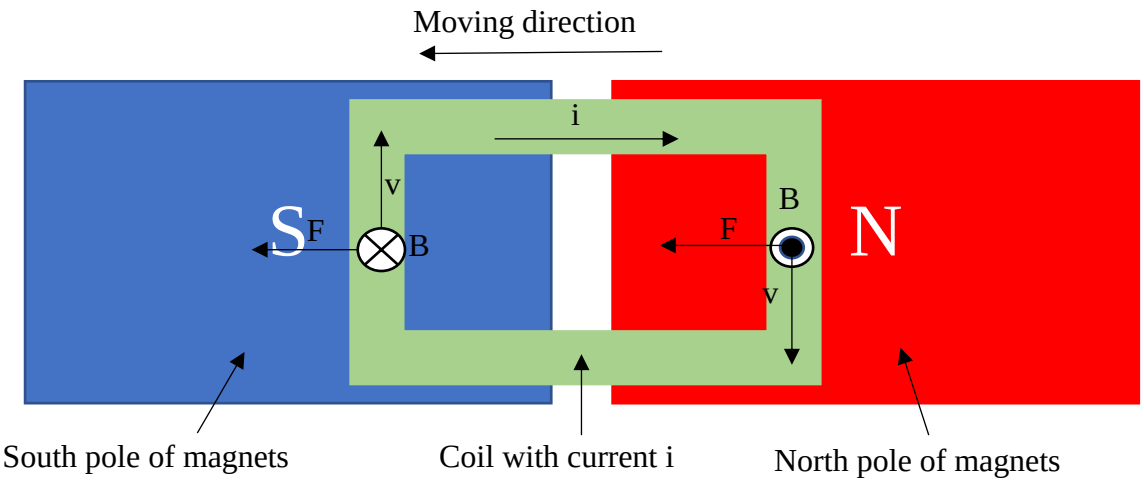

Figure 2: The basic structure of linear motor. Blue and red rectangles are the south and north poles of permanent magnets. Green component is the coil of electromagnets. The current i in magnetic field generates force F as shown in the figure.

While it is true that forces are acting on the top and bottom portions of the coil, each of them can find a force with the same magnitude and opposite direction on the other side. So theoretically, each pair of them can cancel each other. In reality, the magnetic field generated by permanent magnets is not perfectly uniform, and it may result in the incomplete cancellation of

forces. However, this variation is small compared to the net force in the moving direction and can be neglected.

Commonly, the three types of linear motor structures are[7]: mechanical[8], air floatation[9], and magnetic levitation[10]. The mechanical method normally has the simplest structure, lowest cost, easiest maintenance, and is the most used commercially. However, the mechanical contact results in a nonnegligible friction force that decreases both the moving accuracy and energy efficiency. The air floatation method uses high-pressure air to make an air gap between the mover and the stator part. Thus, there is no physical contact between the mover and the stator, and so it would not have high friction as a mechanical structure. However, the high-pressure air will generate a high frequency vibration, which will decrease the moving accuracy of the linear motor. The magnetic levitation seems to be an ideal solution because it has almost zero mechanical friction, high accuracy, and it works well in many special situations. However, it requires superconductor to generate an ultra-high magnetic field, so it is too expensive for most applications.

In this paper, a linear motor with the most fundamental mechanical structure is built. Four C shaped support shells, which included to attempt to reduce friction and increase moving accuracy, are glued to each corner of the mover part. This advanced structure is compared to the fundamental one. Analyses of the motions of both structures are made when the initial input power changes, which can allow analysis more about the system friction and energy efficiency. This comparison may provide suggestions about optimizing the moving accuracy, energy efficiency, and friction reduction.

II. Experimental Methods

2.1 Structure Design

There are two significant factors needed to be considered in designing the motor. One consideration is that the permanent magnet array on the stator must have alternating poles[6]. Otherwise, the generated forces acting on the left and right ends will have opposite directions, and they will cancel each other, which contrasts to the example described in Figure 2. Thus, theoretically, the net force in the movement direction will be smaller than the net force generated with alternating poles.

The other factor is that the current direction in the mover part should alternate when the mover shifts to another magnet. As Figure 3 shows below, moving charges in the wire will flip the direction of thrust force when they move to an opposite magnetic field generated by another permanent magnet. Obviously, if the current goes the same direction all the time, the mover part will move back and forth or stop at an equilibrium point. In order to make it move forward constantly, the direction of current must be flipped when the magnetic field flips.

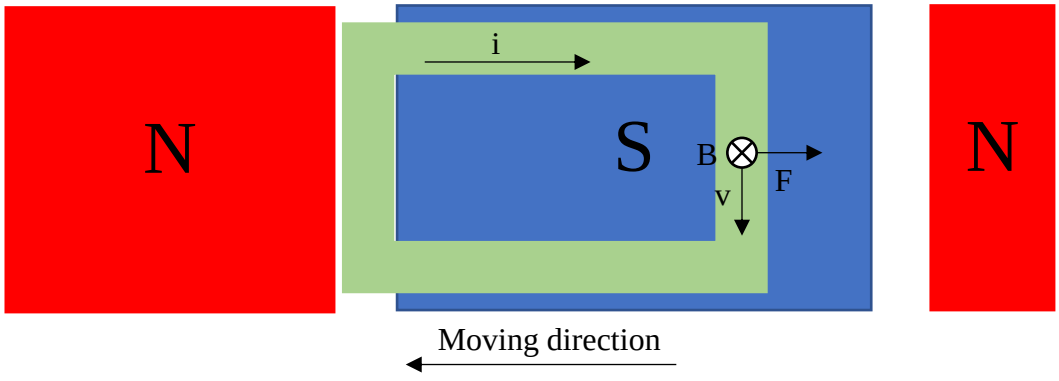

Figure 3: Alternating magnetic force direction. The magnetic force acts on the right side of coil will have opposite direction to the moving direction, if the current direction does not flip with the magnetic pole.

The design of the linear motor made in this experiment is shown in Figure 4. Permanent magnets have dimensions: $0.5'' \times 1'' \times 2''$. Each electrode fixed on the side has a length of 2 inches. The distance between the front and rear parts of the coil is $2.25''$. This distance equals to the length of a permanent magnet plus the separation of a gap. The reason behind this is that, if the separation is far smaller or greater than the length of a magnet, both front and rear ends of the coil will stay in the magnetic fields which have the same direction. In this situation, it is hard to obtain the ideal output force for most of the time. In addition, the separation cannot equal to the length of a magnet, because when the mover shifts to the edge of magnets, both front and rear sides stay in regions with weak strengths of the magnetic field. If the system has a large friction force, the mover may stop at some points like this. The separation is designed to be $2.25''$, and this structure can maximize the generated force and duration of the force, and minimize the mass of the mover as much as possible

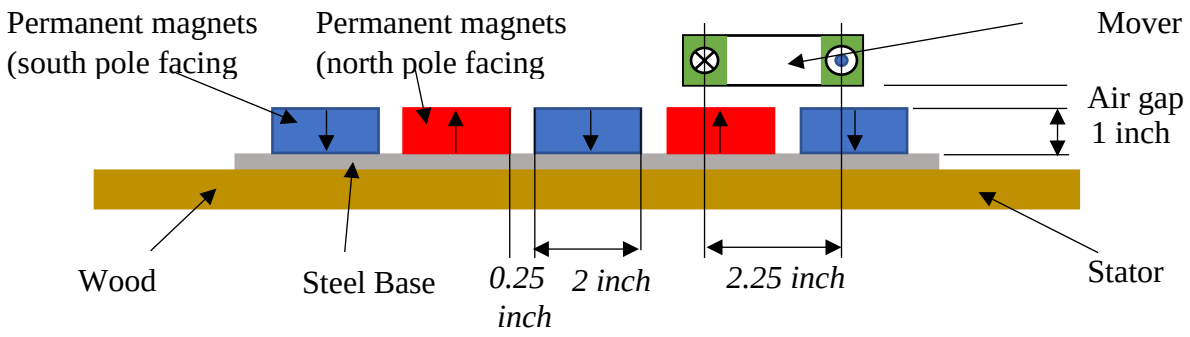

Figure 4: The fundamental structure of a permanent magnet linear motor.

2.2 Stator Part

As Figures 4 and 5 show below, seven permanent magnets with alternating poles are fixed on the steel base. And Figure 6 shows electrodes are made from copper rod and fixed on the inner side of the walls. These rods are connected by wires from the outer side of the walls,

and these wires are connected to a DC power supply. Also, adjacent electrodes will have one grounded, and one has higher voltage; opposite electrodes will have a voltage difference.

Figure 5: Seven permanent magnets on the stator with alternating poles.

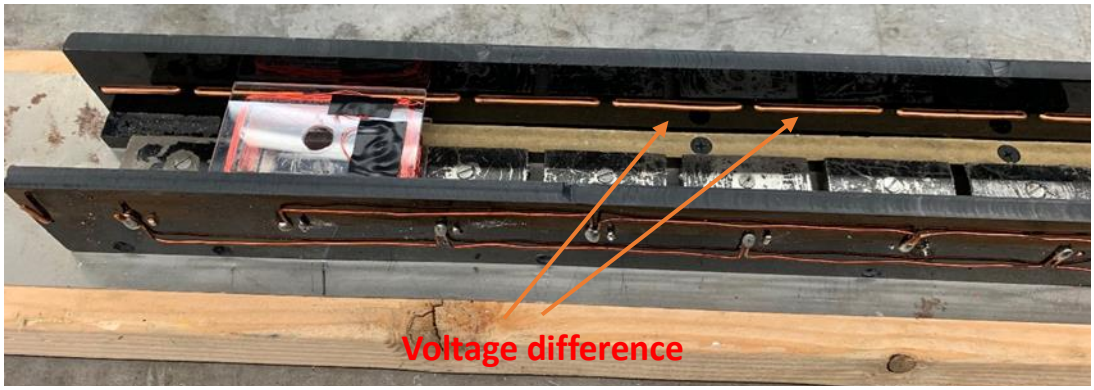

Figure 6: Copper electrodes on the stator. Adjacent and opposite electrodes have voltage difference.

2.3 Mover Part

The body of the mover is made from polymethyl methacrylate. The coil is made from 200 turns of 37-gauge wire. Two thin copper pieces are fixed on both long sides of the mover, and each end of the wire is connected to one of the copper electrodes. PVC electric insulation tape is used to cover all conducting surfaces except the electrode areas. Four C shape support shells are glued on each corner (Figure 7). The support shells hold the copper rods in order to avoid contact between the bottom surface of the mover and permanent magnets. This design is aimed to reduce the friction force and vibration in the vertical direction.

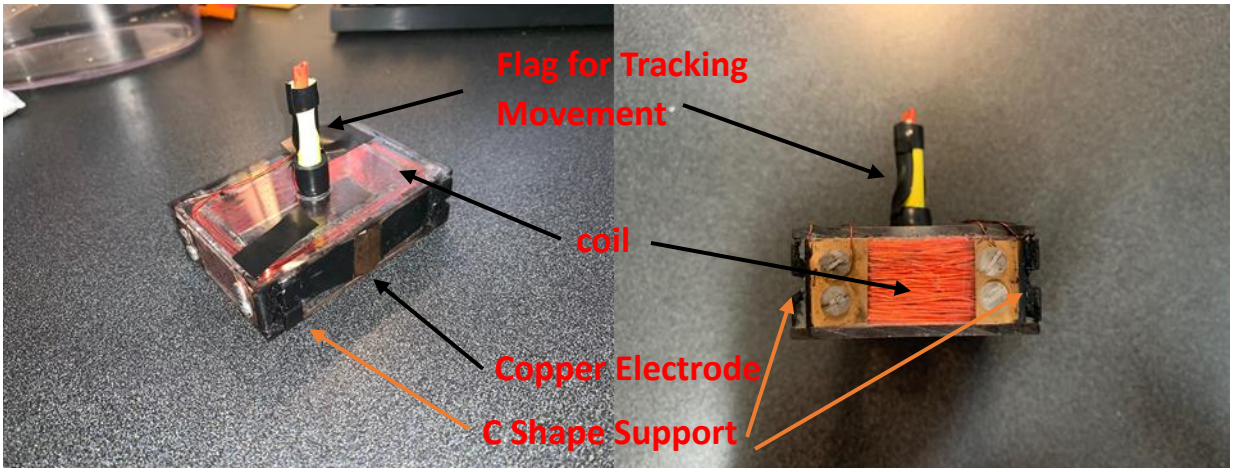

Figure 7: The mover of the linear motor. One copper electrode is mounted on each long side can conduct current.

2.4 Making Measurements

2.4.1 Tracking the Motion of the Mover

In this research, voltage is the single variable that can be changed across the coil. Everything we care about, such as the force generated by the moving charges, the acceleration rate, the output power, the friction of the system and so on, can be calculated and analyzed from the motions of the mover. Thus, in this experiment, the mover (both with the C shells and without the C shells) is tested under 5 different applied voltages (10V, 13V, 16V, 20V, 24V). A camera, capable of making can make videos with 240 frames per second, is placed facing the side of the linear motor and records the motions of the mover. The software Tracker is used to track the changing locations of the small flag (Figure 7) on the mover. All further information can be calculated and analyzed by Excel and Origin (other mathematical tools are listed in the theory section) from the movement curves,

Figure 8 is an example of collecting the location information of the mover part. The location of the mover is tracked frame by frame, and those red circles are the tracked position of

the little red flag on the mover.

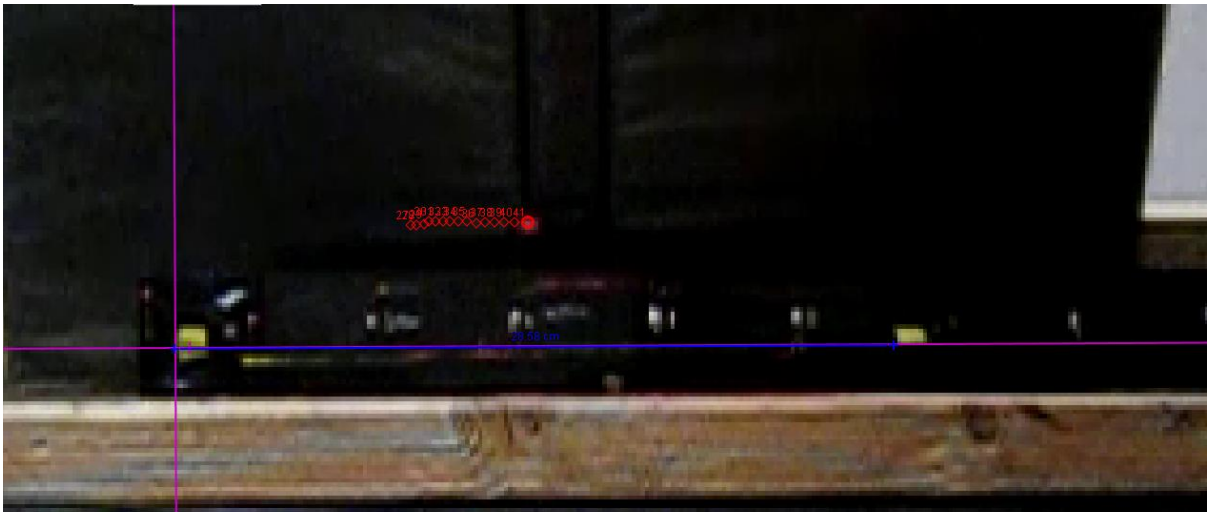

Figure 8: A screen shot of motion analysis of the mover in Tracker software. Yellow marks indicate the starting point (left) and end point(right) of all measurements. Red circles indicate the location of the mover. Purple lines determine the coordinate axes for measurement of this motion.

2.4.2 Measuring the Strength of Magnetic Field

To better model the motion of the mover, the strength of the magnetic field was measured. Thus, a Hall probe is placed at the height of the fixed electrodes (the center height of the coil on the mover), and at the center of the short side of the permanent magnets. The probe is moved from left (Figure 5) to the right, and the strength of the magnetic field is recorded every 5 mm. From these data, it is possible to calculate the theoretical energy gained by the mover and then, estimate the friction force of the system.

III. Theory

3.1 Velocity and Acceleration Approximation

Data points are collected by a camera at a rate of 240 frames/second, means that the time interval between points is $\frac{1}{240}$ s. The mover does not move significantly in this time interval, so it is possible to approximate the velocity as:

$$v = \frac{(x_2 - x_1)}{240} \tag{2}$$

In this equation, v is the velocity of the mover, and $(x_2 - x_1)$ is the position difference between the two frames. However, the videos are taken with 480×360 pixels. Thus, the minimum position difference can be observed in these videos is:

$$\Delta x = \frac{l_{Real}}{N_{Pixel}} \tag{3}$$

l_{Real} represents the real distance of selected length and N_{Pixel} is the number of pixels in that selected length in the videos. The maximum error of position difference shows in one video frame is $\pm 1 pixels$, so, the uncertainty of estimated velocity can be calculated by the equation:

$$\Delta v = \frac{2\Delta x}{240} \tag{4}$$

The multiple 2 is the maximum error of position difference between two frames, which means the measurement is accurate to within $\pm 2 pixels$. To smooth the data and improve the velocity estimate, the three points and five points approximation, from Burden and Faires[11], may be needed to find an approximated velocity.

$$v(t) = \frac{1}{2\Delta t}[-3x(t) + 4x(t + \Delta t) - x(t + 2\Delta t)] \quad (5)$$

$$v(t) = \frac{1}{12\Delta t}[-25x(t) + 48x(t + \Delta t) - 36x(t + 2\Delta t) + 16x(t + 3\Delta t) - 3x(t + 4\Delta t)] \quad (6)$$

In this project, $x(t)$is the position-time curve, *t* is time, and $\Delta t = \frac{1}{240}$ s is the time interval. Ideally, these two equations can reduce the background noise of the original data.

3.2 The Ideal Thrust Force and Motion of the Mover

The thrust force is not continuously generated because of the gaps between electrodes mounted on the walls. These gaps lead to no current goes through the coil, and no force is generated when the mover shifts to the transition points. Thus, for convenience, assuming the generated thrust force and friction force are constant, and the relationship between thrust force, friction and acceleration can be expressed as:

$$F_T = f + ma \quad or \quad a = \frac{F_T - f}{m} \quad (7)$$

Where, $F_T$is the thrust force, f is the friction force, m is the mass of the mover and a is the acceleration rate. Also, the motion of the mover can be simply written as the equation:

$$x = x_0 + v_0 t + \frac{1}{2}at^2 \quad (8)$$

Where x is the position of the mover, x_0 and v_0 are initial position and initial velocity, and t is time.

3.3 Electromagnetic Force

We can use the electromagnetic force equation to calculate the force generated by the current, and the equation is defined as Eq.1. By symmetry, forces acting on the top and bottom sides of the coil (two long sides) will cancel out each other, so they can be ignored. As the movement of charges in front and rear parts is perpendicular to the vertical component of the magnetic field, the net force is in the moving direction, so the cross product can be neglected. Also, by multiplying the turns of the wire, *n*. Eq.1 can be rewritten as:

$$\boldsymbol{F} = nL\boldsymbol{i}\boldsymbol{B} \tag{9}$$

Current is not a variable that can be read from the power supply directly. Using Ohm's law:

$$V = i \times R_{resist} \tag{10}$$

R_{resist} is the resistance of the whole system. Replacing *i*, Eq. 9 becomes:

$$F = \frac{nLVB}{R_{resist}} \tag{11}$$

3.4 Magnetic Field Analysis

Due to the uneven distribution of the magnetic field and friction force, it is hard to measure and discuss the strength of the magnetic field and the work done by a specific force; however, it is possible to assume the magnetic field and force have constant average values in a region, so that the total energy efficiency can be estimated.

Using the law of conservation of energy:

$$K = W - W_f \tag{12}$$

This means that the kinetic energy of the mover, *K*, equals the work done by the current in the coil, *W*, minus the energy loss of against friction force, W_f.

As work is equal to the force times the moving distance on the force direction, the equation can be rewritten in a more general form:

$$\frac{1}{2}mv^2 = \int 2\frac{nLVB(x)}{R_{resist}}\,dx - \int f\,dx \tag{13}$$

In this equation, *m* is the mass of the mover, 2 represents both the front and rear sides of the mover, *v* is the velocity of the mover, and *f* is the friction force. Assuming B and f are constant values, Eq. 11 becomes:

$$\frac{1}{2}mv^2 = \frac{nLVB}{R_{resist}}\,x - fx \tag{14}$$

In order to cancel out the friction terms, substituting two velocities, v_1 and v_2, from different trials at the same position can help in calculating the value of B.

$$\frac{1}{2}m(v_2^2 - v_1^2) = \frac{nLBx}{R_{resist}}\,(V_2 - V_1)\ \ or\ \ B = \frac{\frac{1}{2}mR_{resist}(v_2^2 - v_1^2)}{nLx(V_2 - V_1)} \tag{15}$$

3.5 Acceleration and Friction Analysis

Relating input voltage and magnetic field to the acceleration rate can help in exploring more about acceleration and friction force. Thus, substituting Eq. 9 into Eq. 7, and reorganizing parameters.

$$a = \frac{nLB}{R_{resist}m}V - \frac{f}{m} \tag{16}$$

3.6 Energy Transfer Rate and Efficiency of the System

The kinetic energy gained by the mover is:

$$K = \frac{1}{2}mv^2 \tag{17}$$

And the work done by the thrust force can be calculated from Eq.11:

$$W_T = Fd \tag{18}$$

$$W_T = \frac{nLVB}{R_{resist}}\, d \tag{19}$$

Thus, the energy transfer rate is:

$$R = \frac{K}{W_T}\ \times 100\% \tag{20}$$

Total energy supplied by the DC power supply can be written as:

$$E = iVt \tag{21}$$

Again, the current cannot be read directly, rewriting Eq. 18 with term V, R_{resist} and t:

$$E = \frac{tV^2}{R_{resist}} \tag{22}$$

Thus, the total energy efficiency of the linear motor can be calculated by Eq.23:

$$\eta = \frac{K}{E} \times 100\% \tag{23}$$

IV. Result and Analysis

4.1 Velocity Analysis

The measured resistance of the system is 7.9 ohm, so the applied voltage 10V, 13V, 16V, 20V, and 24V, means those input powers are 12.66W, 21.40W, 32.41W, 50.63W, 72.91W. As Figure 9 shows, regardless of the applied voltage, the mover is moving monotonically. In other words, the separation of $2.25''$ was designed correctly since the coil did not move back and forth. It is also worthwhile to notice that for higher power applied to the system, the position line has a sharper slope. This result is reasonable because the greater current will do more work on the mover when it goes through the magnetic field.

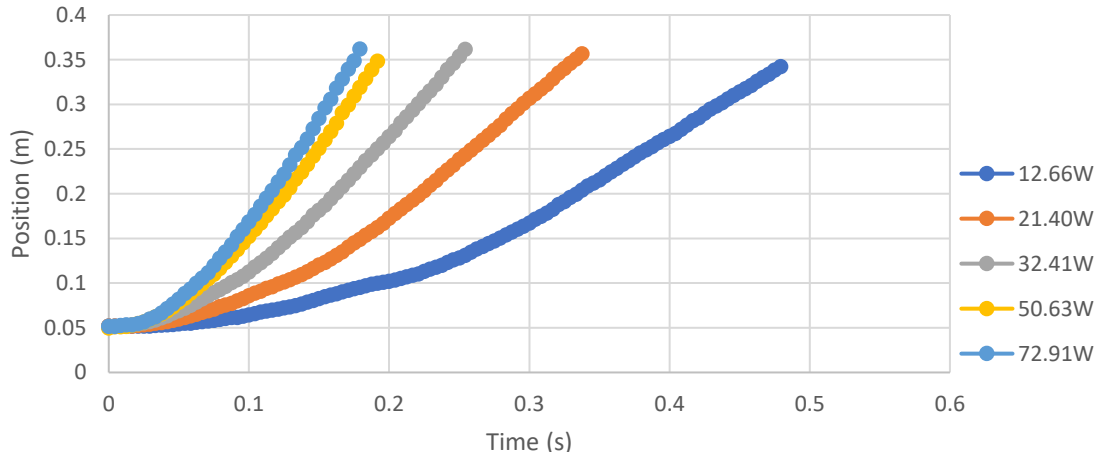

Figure 9: The changing positions of the mover (with C shape support shell) versus time. Different colors denote the different input powers.

By using Eq. 2, figures of instantaneous velocity versus time can be calculated. These results are plotted in Figure 10. For all trials, velocity data points are scattered due to small noise in the position graphs.

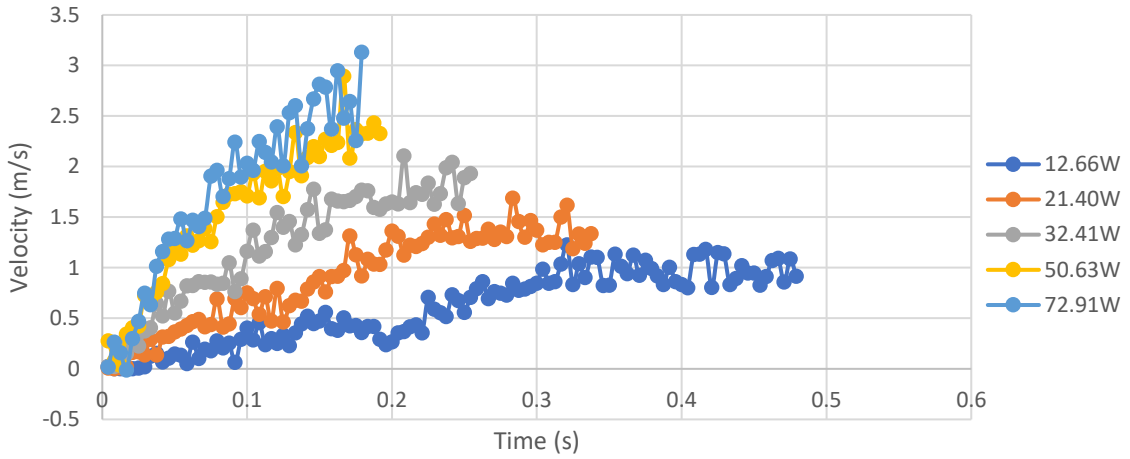

Figure.10: Velocity of the mover (with C shape support shell) versus time, showing increased acceleration for higher powers.

To improve these calculations for velocity, 3 points and 5 points approximations (Eq. 3 and 4) were tested, as shown in Figures 11 and 12. Typically, these alternate forms are used to remove random noise. However, the more points used in the approximation, the more the data line oscillates. Thus, if the higher orders do not improve, the noise may be part of the experiment. For instance, perhaps the vertical vibration of the mover introduces noise.

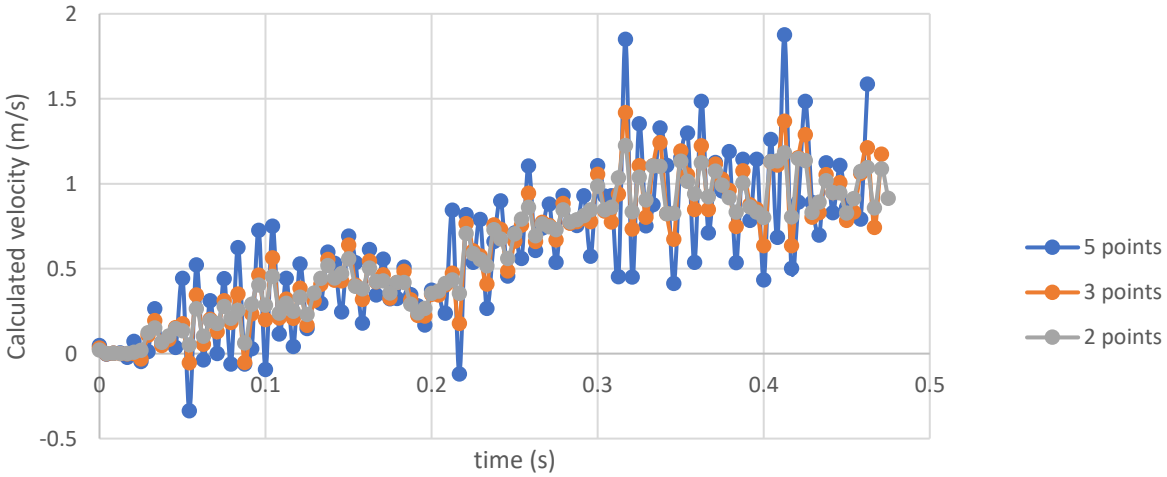

Figure 11: Determination of velocity using three different approximation methods, as described in the text. The applied power was 12.66 W

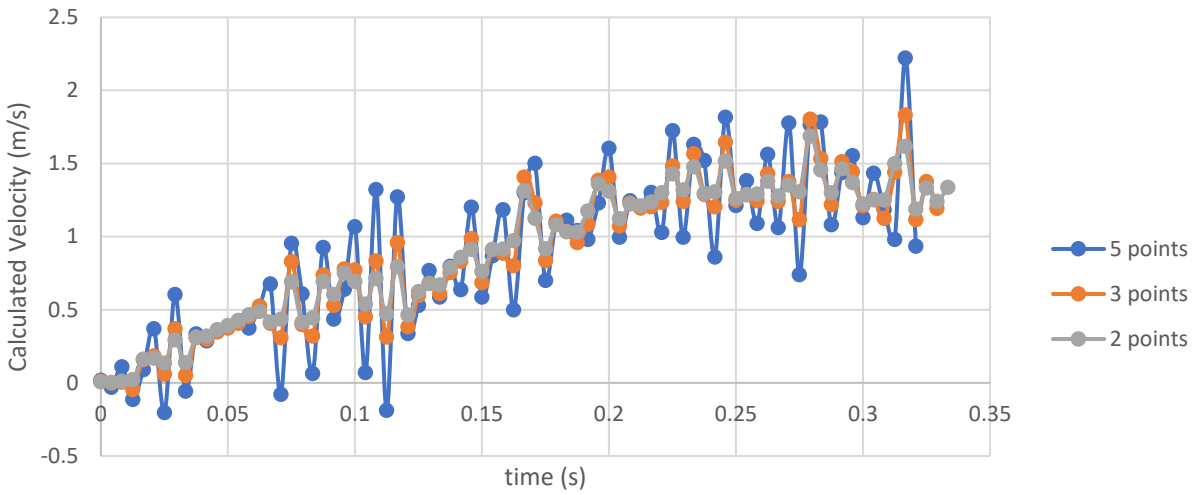

Figure 12: Determination of velocity using three different approximation methods, as described in the text. The applied power was 21.40 W

Because these calculations of velocity are so noisy, a different approach is used to solve this problem. It is clear that fitting data points to Eq. 8 and solve for fitting parameters can provide better results.

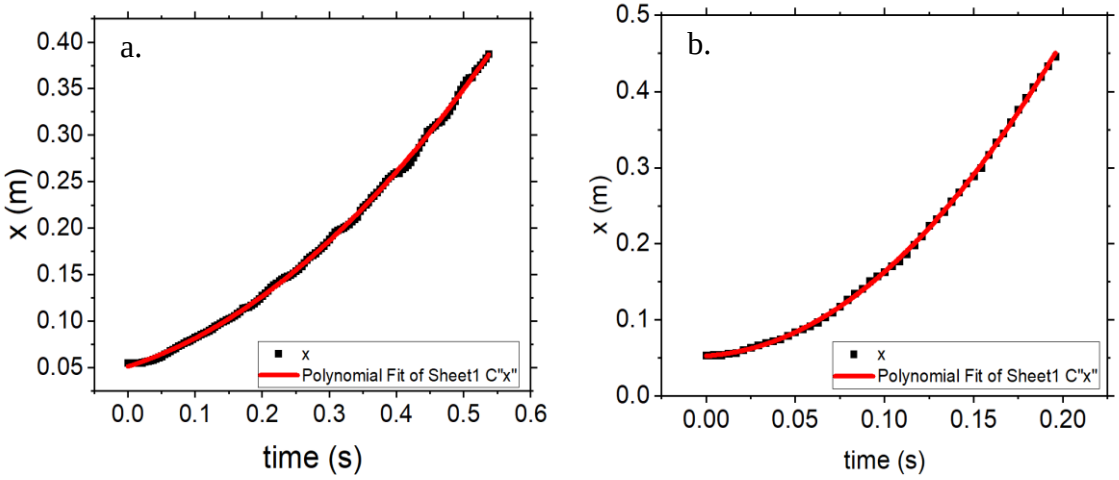

Figure 13: Example graphs of fitting lines to original data. (a) Without C shell and 10 V applied voltage, (b) Without C shell and 24 V applied voltage.

4.2 Acceleration and Friction Force in Two Structure

All motion is fitted to the Eq. 8, which allows one to fit *a* (acceleration) under different initial conditions, so all acceleration values are pulled out and forming Figure 14:

Both lines should fit Eq. 16. The slope of the red line (no C shell) is 1.34m/Vs^2 , and the y-intercept is -11.86 m/s^2 . Also, the slope of the blue line (with C shell) is 0.907 m/Vs^2, and the y-intercept is -6.82 m/s^2. Obviously, the y-intercepts relate to friction force directly, with C support shells, the friction force decreases significantly. However, the slop shows that without the C shells, the mover has a higher acceleration rate. In this experiment, *n*, *L*, *m* and R_{resist} are constant parameters, the different slopes can only mean that the strength of magnetic field changes. One possibility is that, without the C shells, the mover contacts the permanent magnets directly, so the mover is closer to the magnets and it results in a stronger magnetic field, which would generate a stronger force and acceleration.

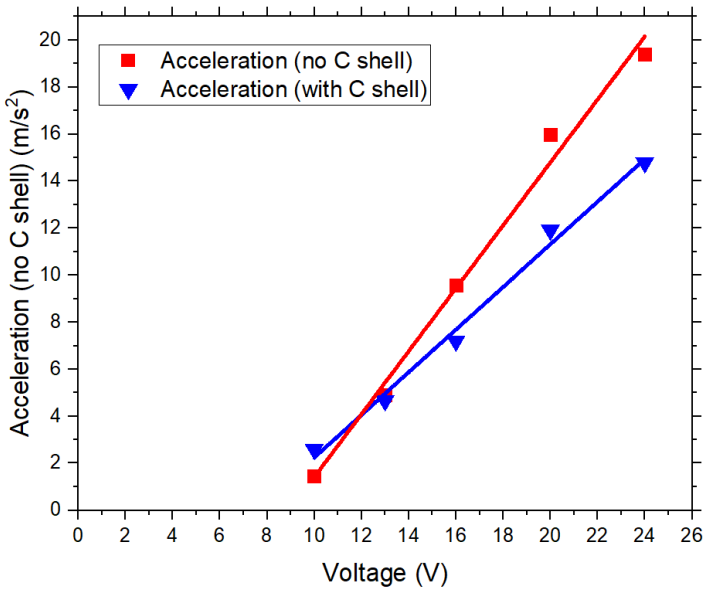

Figure 14: Acceleration rates of the linear motor with different initial conditions. Red line shows data collected without the C shell. bule line is data with C shell.

4.3 Magnetic Field Analysis

4.3.1 Measured Magnetic Field

The strength of the magnetic field is measured by a Hall probe in the previous section. Plotting these data points in one figure (Figure 15). The dashes represent the transitions in which coils are not touching electrodes (see section 2). However, since the current *i* and magnetic field *B* are both reversed as the motor touches different electrodes, according to Eq. 9, the thrust force keeps towards the same direction all the time. For convenience, assume that all magnetic field values are absolute values, and the current runs in the same direction. Thus, the magnetic field can be plotted, as shown in Figure 16.

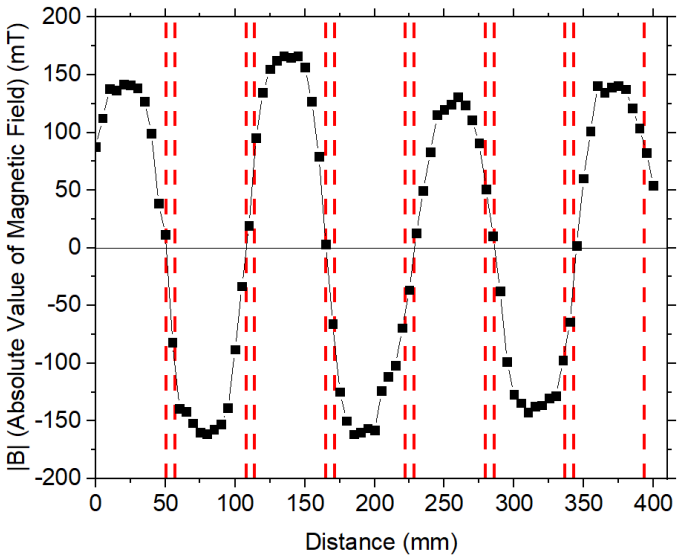

Figure 15: The measured magnetic field. The dashes represent the small gaps in which the mover is not connected to current sources.

The average value of the strength of the magnetic field can be calculated by the mathematical method of summing up the area under the curve, and then, dividing the area by the total distance. Using software Origin to calculate the total area, and the average value of the magnetic field is 0.102T.

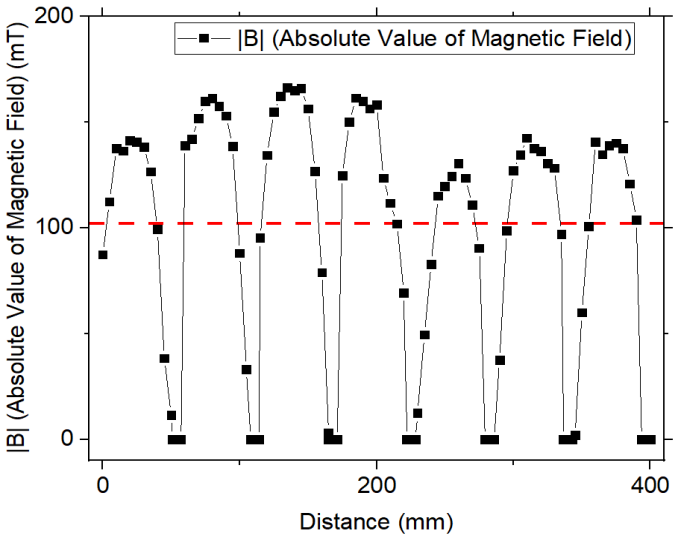

Figure 16: The absolute value of the magnetic field shown in figure 15. Dashed line represents average field.

4.3.2 Calculated Magnetic Field

In order to calculate the energy efficiency of this system, the average value of the strength of the magnetic field is required. Substituting L = 0.042m, m = 0.083 kg, x = 0.25m , R_{resist} = 7.9ohm and two velocities from different trials at a similar position into Eq. 15.

Table.1: The velocity of the mover at a similar position from different trials.

	Position(m)	Velocity(m/s)
1	0.3017	0.8924
2	0.3066	1.371
3	0.3005	1.724
4	0.2993	2.083
5	0.3057	2.372

The calculated values of the strength of the magnetic field are consistent between trials, and the average value is 0.028 T.

4.3.3 Magnetic Field Difference Analysis

The magnetic field is calculated from both the motion of the mover and the measurements of the magnetic field by using a Hall probe, but the two results do not match well. However, both values are in the same order of magnitude, which is encouraging that both values somewhat agree on each other. This difference may be a piece of evidence to show that something else changes when the mover is moving. Considering that when the mover shifts to these gaps, neither the magnetic field in this region (which is too small in Figure 16) nor the inject current (which is zero) would affect the calculation of average magnetic field. Thus, the problem is more likely to exist in the process of calculating. In Eq. 16, n, m and L are measured directly, but the resistance, R_{resist}, of the circuit is measured by a multimeter. Thus, there are two considerations about the resistance of the linear motor. Firstly, comparing to the current (A scale) goes through the circuit, the current injected by multimeter is too small (mA scale) to generate enough heat to increase the resistance of the wire. However, the wire used to make the coil is so thin and the current provided by the DC power supply is large, so that the coil will generate much more heat, and the resistance of the wire should be higher than the reading of the multimeter. Secondly, the resistance measurement is taken when the mover is stopped inside the linear motor. However, when the mover is moving, electrodes may not contact well, which would result in a bad electrical conductivity. All of those possibilities should be considered in future research because it does affect the analysis of energy efficiency.

4.4 Efficiency Analysis

The work done by the DC power supply can be found by Eq. 22, and then using Eq. 23 to find out the energy efficiency of the system. Figure 17 shows an increase in total energy efficiency as the input power increases. Also, the input power and energy efficiency have an increasing linear relationship when the input power less than 50W. This result should be reasonable, because the work done against the system friction is nearly constant, so the efficiency should increase linearly to the work done by the power supply. Considering the current capacity of the wire on the coil (the maximum current for 37-gauge wire is 3 A), readings with higher input powers may not be able to be obtained on this device.

However, the concave down trend at higher power may suggest that more and more electric energy transfers to heat in conducting wires. This heat increases the resistance of the circuit, which results in an efficiency loss. In order to eliminate the energy loss in conducting wires, use the ratio of the kinetic energy of the mover to the input energy as the energy transfer rate.

The work done by the thrust force can be found by Eq. 19, and then substituting the work into Eq. 20, the energy transfer rate can be obtained. Figure 18 shows that the energy transfer rate seems to reach a maximum value when the current reaches a certain level. This value may represent the maximum energy efficiency of the system. However, due to the non-neglectable resistance, this value may never be achieved. Thus, the maximum transfer rate and energy efficiency of this linear motor system are about 67% and 29% respectively.

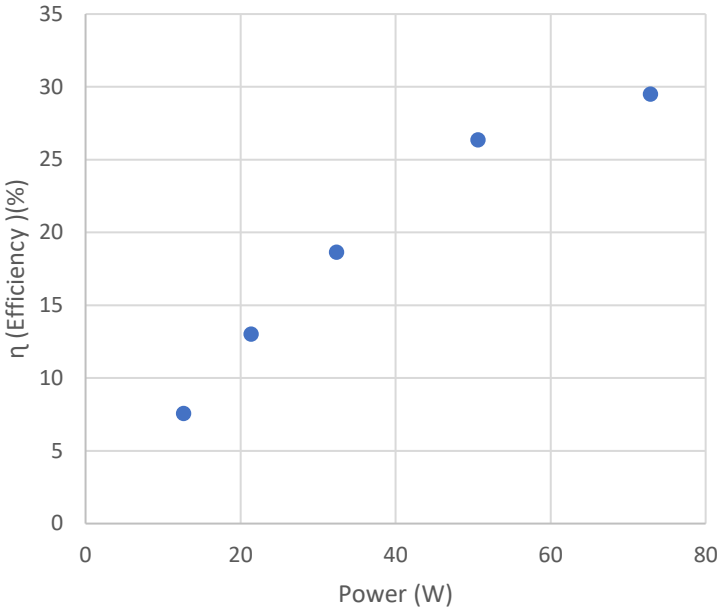

Figure 17: The total efficiency of the linear motor. The energy efficiency increases linearly with applied power less than 50W.

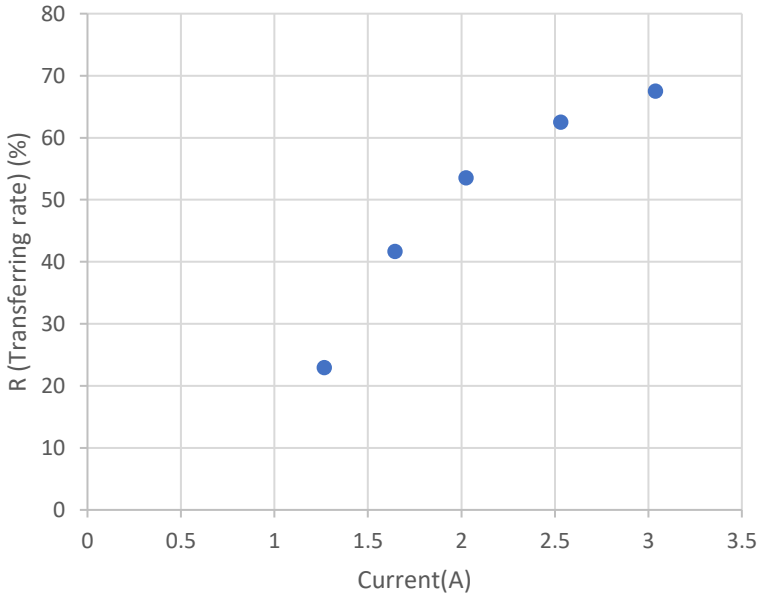

Figure 18: The Energy transfer rates increase with current, suggesting a better efficiency.

4.5 Uncertainty

4.5.1 Approximated Velocity Error

To calculate the position uncertainty, Eq. 3 is used, finding about 1.1mm. Eq. 4 is used to calculate the velocity uncertainty, which is about 0.00917mm/s. As both uncertainties are tiny, they can be ignored in the calculation.

4.5.2 Friction force

In previous sections, magnetic field and friction are assumed to be an average, constant, value. However, the truth is that they are not constant. One of the reasons is that every time the mover shifts, it does not take the exact same path. Plotting the motion of the mover in two dimensions, the moving path can be graphed as:

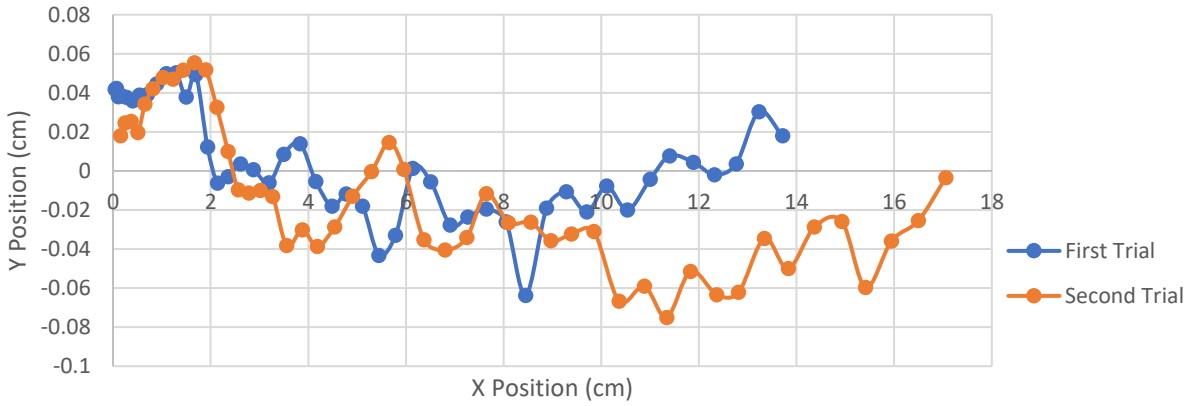

Figure 19: The moving paths of the mover in two trials. It is showing some parts the paths have some overlaps, but the majority parts are distinct.

Thus, this assumption about contact friction, in the theory section, should not be reliable. Also, the analysis in section 4.2 shows that the work done against friction force is not negligible when the input power is low. According to Figure 17, for the first two trials, energy efficiency is

extremely low. In other word, most of the energy is transferred to heat when conducting and against friction force, so any position measurements on these trials should have a nonnegligible noise.

4.5.3 Fluctuation

Due to the unevenly distributed magnetic field, the force acting on the mover part is not only in the moving direction, but also, there are many force components towards the vertical direction. As the figure below shows, the mover without the C shape support shells is oscillating while moving, and the maximum oscillation is about 6mm. This fluctuation is not observable by eyes when testing the mover with C shells, but it does cause the errors when approximating its motions in section 4.1.

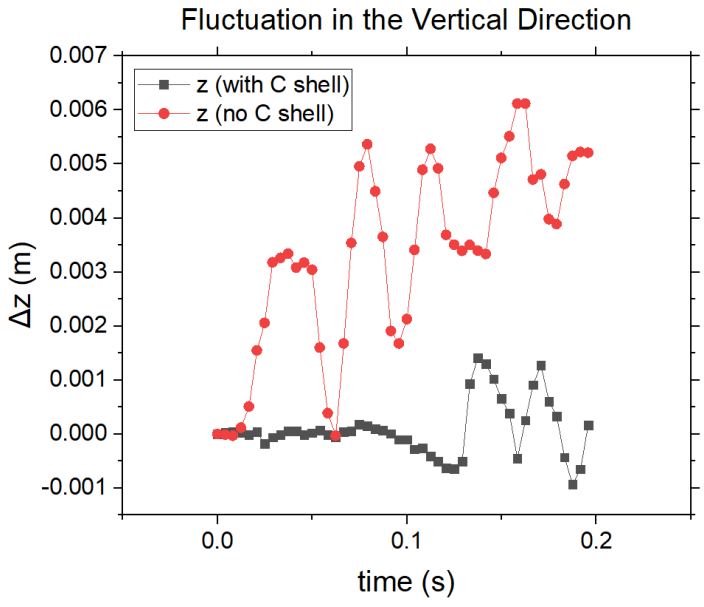

Figure 20: Measurements of the motion on the vertical direction (without C shell). The maximum difference in *z* direction is close to 6 mm.

V. Conclusion

In this paper, with the goal of improving the structure of a mechanical contact linear motor in order to maximize the energy efficiency of the motor. Various designs for permanent magnet linear motors which are able to output more thrust force and have higher net efficiency were investigated. Through this project, several suggestions about reducing friction force and increasing energy efficiency in small permanent magnets linear motor system are provided, which should be considered by any future researchers.

The C shape support shells can reduce the oscillation in the vertical direction significantly, which increases the stability of movement. In addition, the C shape support shells avoid direct contact on the bottom surface, which reduces the friction and increase the total energy efficiency of the system. Designing the separation between the front and the rear sides of the coil to equal the length of a magnet and one gap brings in many advantages. This structure maximizes the thrust force and shrinks the size and weight to a minimum, which leads to a higher thrust force and acceleration rate.

Another consideration, mentioned in section 4.3.3, is that electrical resistance is a concern. The linear motor has direct contact electrodes, which may affect how well the current conducts. In addition, due to the large current, a lot of heat is generated, which will increase the resistance of conducting wire. Thus, the resistance of the circuit is changing when the mover is accelerating.

This prototype of linear motor achieved the maximum efficiency of 30%, and 79% energy transferring rate (energy gained versus work done by moving charge). And for future research, researchers may want to minimize the size of permanent magnets in order to achieve a

more evenly distributed magnetic field. A thick wire made coil may help in decreasing resistance and increasing efficiency. Also, it is necessary to smooth every contact surface, so that the linear motor has a higher moving accuracy and energy efficiency.

Bibliography

1. Jufer, M. Electric drive: design methodology. (2010).
2. Aoyama, Y. *et al.* Development of High-Acceleration Linear Motor to Realize Resource Saving and High Productivity. *Electr. Eng. Japan (English Transl. Denki Gakkai Ronbunshi)* **202,** 55–63 (2018).
3. Industry, N. & Province, N. Electric Machine Technology Needs Analysis Of the Linear Motor ZHAO Yu-ping. **491,** 1138–1141 (2014).
4. Quan, L. I. U. & Yuan, F. E. I. Design and Manufacture of a Unilateral Permanent Magnet Linear Motor for Assembly. **500,** 543–546 (2014).
5. Qin, C., Zhang, C. & Lu, H. H-shaped multiple linear motor drive platform control system design based on an inverse system method. *Energies* **10,** (2017).
6. Omura, M., Shimono, T. & Fujimoto, Y. Development of Semicircular Tubular Coreless Linear Motor and Its Motion Control. **195,** 246–257 (2016).
7. Xing, F., Kou, B., Zhang, L., Wang, T. & Zhang, C. Analysis and Design of a Maglev Permanent Magnet Synchronous Linear Motor to Reduce Additional Torque in dq Current Control. *Energies* **11,** 556 (2018).
8. Cao, R., Cheng, M. & Zhang, B. Speed Control of Complementary and Modular Linear Flux-Switching Permanent Magnet Motor. *IEEE Trans. Ind. Electron.* **62,** (2015).
9. Mori, S., Hoshino, T., Obinata, G. & Ouchi, K. Air-bearing Linear Actuator for Highly Precise Tracking. *IEEE Trans. Magn.* **39,** (2003).
10. Guo, Y. *et al.* Design and Analysis of a Prototype Linear Motor Driving System for HTS Maglev Transportation. **17,** 2087–2090 (2007).
11. Burden, R. & Faires, D. *Numerical Analysis*. (1997).
12. [1]Schnibbi678. "Linear Motor Principle". *Wikimedia, Jan. 7.* 2013, https://commons.wikimedia.org/wiki/File:Linearmotorprinzip.png